SUPPLEMENTARY ONLINE MATERIAL

No	NDB ID	Method	Sequence of first strand	Comments*,**	Subset§
1	BD0001	x-ray	A-C-C-G-A-C-G-T-C-G-G-T	Spermine	a,b
2	BD0002	x-ray	A-C-C-G-A-C-G-T-C-G-G-T	spermine	a,b
3	BD0003	x-ray	A-C-C-G-G-T-A-C-C-G-G-T	spermine	a,b
4	BD0005	x-ray	C-G-C-G-A-A-T-T-C-G-C-G	spermine	b
5	BD0015	x-ray	C-C-G-C-C-G-G-C-G-G	spermine	a,c,e
6	BD0023	x-ray	C-C-A-G-T-A-C-T-G-G	spermine	c,d
7	BD0028	x-ray	C-C-G-C-T-A-G-C-G-G	(not reported)	a,c,e
8	BD0029	x-ray	C-G-C-G-A-A-T-T-C-G-C-G	spermine	b
9	BD0033	x-ray	C-C-A-A-C-G-T-T-G-G	streptonigrin**, no sp or cohex	c,d
10	BD0034	x-ray	C-C-A-A-C-G-T-T-G-G	streptonigrin**, no sp or cohex	c,d
11	BD0035	x-ray	C-C-A-G-C-G-C-T-G-G	streptonigrin**, no sp or cohex	c,d
12	BC0036	x-ray	C-C-A-G-C-G-C-T-G-G	streptonigrin**, no sp or cohex	c,d
13	BD0041	x-ray	C-G-C-G-A-A-T-T-C-G-C-G	spermine	b
14	BD0047	x-ray	G-C-A-A-A-C-G-T-T-T-G-C	spermine	a,b
15	BD0051	x-ray	C-C-T-T-T-A-A-A-G-G	spermine	c,e
16	BD0052	x-ray	A-C-C-G-A-A-T-T-C-G-G-T	spermine	a,b
17	BD0057	x-ray	C-G-C-T-T-A-T-A-T-G-C-G	spermine	b
18	BD0077	x-ray	C-C-G-T-T-A-A-C-G-G	spermine	c,e
19	BD0079	x-ray	C-C-A-G-C-G-C-T-G-G	spermine	c,e
20	BD0080	x-ray	C-C-G-T-C-G-A-C-G-G	spermine	a,c,e
21	BD0081	x-ray	C-C-G-C-C-G-G-C-G-G	spermine	a,c,e
22	BD0082	x-ray	C-C-G-A-T-A-T-C-G-G	spermine	a,c,e
23	BD0086	x-ray	C-C-G-C-T-A-G-C-G-G	spermine	a,c,e
24	BD0087	x-ray	C-C-G-A-A-T-T-C-G-G	spermine	c,e
25	BD0090	x-ray	G-C-A-G-A-C-G-T-C-T-G-C	cobalt hexamine	a,b
26	BDJ017	x-ray	C-C-A-G-G-C-C-T-G-G	no sp or cohex	c,d
27	BDJ019	x-ray	C-C-A-A-C-G-T-T-G-G	no sp or cohex	c,d
28	BDJ025	x-ray	C-G-A-T-C-G-A-T-C-G	no sp or cohex	a,c,d
29	BDJ031	x-ray	C-G-A-T-T-A-A-T-C-G	spermine	c,e
30	BDJ036	x-ray	C-G-A-T-A-T-A-T-C-G	spermine	a,c,e
31	BDJ037	x-ray	C-G-A-T-A-T-A-T-C-G	spermine	a,c,e
32	BDJ039	x-ray	C-C-G-G-C-G-C-C-G-G	no sp or cohex	a,c,d
33	BDJ051	x-ray	C-A-T-G-G-C-C-A-T-G	spermine	a,c,e
34	BDJ052	x-ray	C-C-A-A-G-C-T-T-G-G	no sp or cohex	c,d
35	BDJ055	x-ray	C-C-A-T-T-A-A-T-G-G	no sp or cohex	a,c,d
36	BDJ060	x-ray	C-T-C-T-C-G-A-G-A-G	no sp or cohex	a,c,d
37	BDJ061	x-ray	C-C-A-C-T-A-G-T-G-G	spermine	c,e
38	BDJ069	x-ray	C-G-C-A-A-T-T-G-C-G	no sp or cohex	a,c,d
39	BDL001	x-ray	C-G-C-G-A-A-T-T-C-G-C-G	spermine	b
40	BDL002	x-ray	C-G-C-G-A-A-T-T-C-G-C-G	(not reported)	b
41	BDL006	x-ray	C-G-C-A-A-A-A-A-A-G-C-G	spermine	b
42	BDL007	x-ray	C-G-C-A-T-A-T-A-T-G-C-G	spermine	b
43	BDL020	x-ray	C-G-C-G-A-A-T-T-C-G-C-G	spermine	b
44	BDL028	x-ray	C-G-T-G-A-A-T-T-C-A-C-G	spermine	b
45	BDL029	x-ray	C-G-T-G-A-A-T-T-C-A-C-G	spermine	b
46	BDL038	x-ray	C-G-C-A-A-A-T-T-T-G-C-G	spermine	a,b
47	BDL042	x-ray	C-G-T-A-G-A-T-C-T-A-C-G	spermine	a,b
48	BDL059	x-ray	C-G-C-G-T-T-A-A-C-G-C-G	spermine	b
49	BDL078	x-ray	C-G-C-G-A-T-A-T-C-G-C-G	spermine	b
50	BDL084	x-ray	C-G-C-G-A-A-T-T-C-G-C-G	spermine	b

1	132D	NMR	G-C-C-G-T-T-A-A-C-G-G-C		
2	1AFZ	NMR	G-G-C-A-G-G-T-G-G-T-G		
3	1AGH	NMR	C-G-G-A-C-A-A-G-A-A-G		
4	1BWT	NMR	G-C-G-A-A-T-T-C-G-C		
5	1CS2	NMR	C-T-A-C-T-G-C-T-T-T-A-G		
6	1D19	NMR	G-T-A-C-G-T-A-C		
7	1D20	NMR	T-C-T-A-T-C-A-C-C-G		
8	1D68	NMR	G-C-G-T-A-T-A-C-G-C		
9	1DUF	NMR	C-G-C-G-A-A-T-T-C-G-C-G		
10	1FZX	NMR	G-G-C-A-A-A-A-A-A-C-G-G		
11	1G14	NMR	G-G-C-A-A-G-A-A-A-C-G-G		
12	1G80	NMR	G-C-G-T-A-C-G-C		
13	1GIP	NMR	C-G-C-G-A-A-T-T-C-G-C-G		
14	1IR5	NMR	C-A-C-T-A-C-T-C-T-T-T-G-T-A-G-T-G		
15	1K8J	NMR	C-C-A-G-G-A-G-A-T-T-C-C-A-C		
16	1K9L	NMR	T-A-T-G-A-G-C-G-C-T-C-A-T-A		
17	1KBD	NMR	C-T-G-G-G-G-A-C-T-T-T-C-C-A-G-G		
18	1KKV	NMR	C-C-A-C-G-C-G-T-G-G		
19	1LAI	NMR	C-G-C-G-G-T-G-T-C-C-G-C-G		
20	1NAJ	NMR	C-G-C-G-A-A-T-T-C-G-C-G		
21	1OPQ	NMR	G-C-G-A-G-A-T-C-T-G-C-G		
22	1RVH	NMR	G-C-A-A-A-A-T-T-T-T-G-C		
23	1RVI	NMR	C-G-T-T-T-A-A-A-A-C-G		
24	1X2S	NMR	G-A-C-T-G-T-A-C-A-G-T-C		
25	2DAU	NMR	C-G-C-G-A-A-T-T-C-G-C-G		
26	3KBD	NMR	C-T-G-C-T-C-A-C-T-T-T-C-C-A-G-G		

Table S1. Oligomers selected from NDB[†] for constructing DNA-*cry* and DNA-*nmr* models.

[†] http://ndbserver.rutgers.edu

* While commonly used in oligomer crystallization buffers, spermine (sp) or cobalt hexamine (cohex) are known to bind and precipitate DNA from solution [Bloomfield, V.A., Crothers, D.M., and Tinoco, I., Jr. (2000) Nucleic Acids: Structures, Properties, and Functions; University Science Books, Sausalito, CA]. Because their effect on DNA structure in crystals cannot be excluded *a priori*, the presence or absence of these ions in the crystallization buffer is noted in this column.

** In several decamer structures, streptonigrin was used in the crystallization buffer, as noted in the last column. Under the reported crystallization conditions (no transition metal ions), streptonigrin has low DNA binding affinity [Rao, K.V. (2006) Interaction of streptonigrin with metals and with DNA; *J. Pharm. Sci.* **68**, 853-856]. Hence, we did not exclude these oligomers from our analysis, in contrast to oligomers co-crystallized with DNA-binding drugs.

[§] For the analysis of helical coherence, x-ray structures were separated into the following subsets: a – oligonucleotides with no kinks visible upon examination with a 3D viewer, b – all dodecamers, c – all decamers, d – all decamers without spermine or cobalt hexamine present in the crystallization buffer, and e – decamers crystallized with spermine or cobalt hexamine.

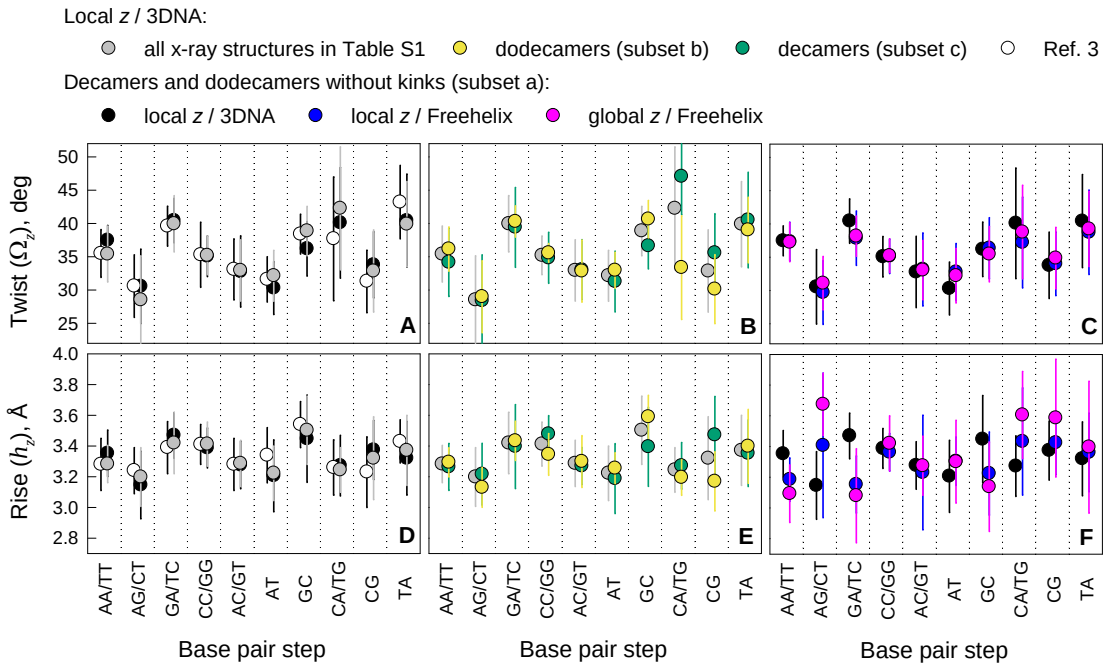

Figure S1. **Average twist (A-C) and rise (D-F) values for the 10 possible base pair steps in oligomer crystals.** The average twist and rise extracted with 3DNA (local *z* / 3DNA) from the full set of 50 crystal structures (Table S1) used for this study were similar to the published data [Ref. (3) updated at http://rutchem.rutgers.edu/~olson/ave_dpn.html]. The twist and rise values were also similar in dodecamer and decamer subsets of Table S1 structures, except for the CA/TG step known to exhibit bimodal distribution (3). As shown in Ref. (41) the values of the twist but not the rise were also similar when extracted with Freehelix98 in a local reference frame (local *z* / Freehelix) or with respect to the global oligonucleotide helical axis (global *z* / Freehelix).

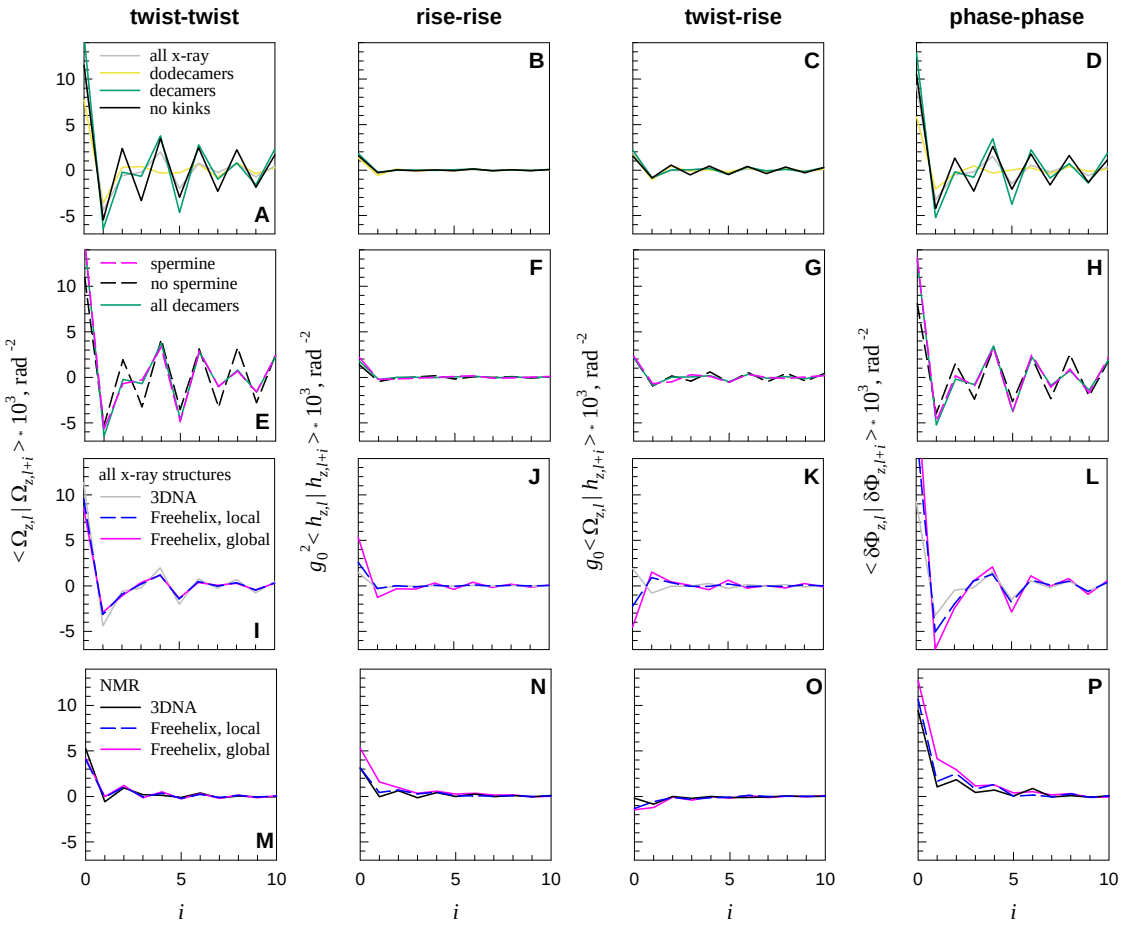

Figure S2. **The twist, rise, twist-rise, and helical phase correlations in DNA-*cry* models based on different subsets of oligonucleotides with local *z*/3DNA parameters (A-H) and the same correlations in DNA-*cry* and DNA-*nmr* models based on full sets of oligonucletides with local *z*/3DNA, local *z*/Freehelix, or global *z*/Freehelix parameters (I-P).** The panels M-P are the same as in the main text. DNA-*cry* models were generated as described in the main text from the full set of 50 structures listed in Table S1, 22 of these structures with no visible kinks (subset a), 22 dodecamer structures (subset b), 28 decamer structures (subset c), 13 decamer structures with no spermine or cobalt hexamine in the crystallization buffer (subset d), and 15 decamer structures with spermine in the crystallization buffer (subset e). The correlation functions were calculated as for Figure 3 of the main text. The main features of DNA-*cry* correlation functions (e.g., strong anticorrelation between consecutive steps) were found to be qualitatively similar in all subsets. The saw-tooth correlation pattern was most pronounced in oligonucleotides with no visible kinks, indicating that kinks tend to disrupt correlations between consecutive steps. The amplitude and range of the twist and helical phase variations were larger in decamers compared to dodecamers. The difference may be related to less constrained crystal packing of decamers, which stack end-to-end akin to uninterrupted long molecules, while dodecamers are more constricted (see, e.g., Ref. (1) in the main text). No statistically significant effect of spermine on the correlation functions was apparent, but the sampling based on reported structures might not be sufficient for a definite conclusion. The correlations in any of the DNA-*cry* subsets were qualitatively different from DNA-*nmr*, as discussed in the main text.

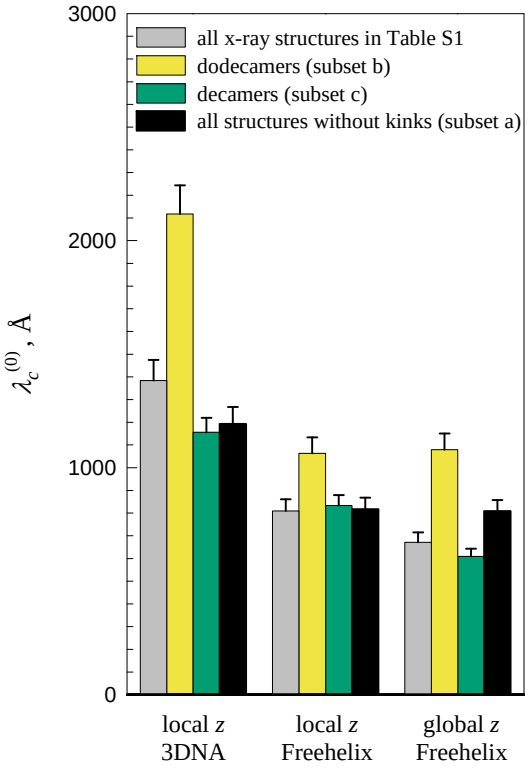

Figure S3. **Intrinsic helical coherence length $\lambda_c^{(0)}$ of DNA-*cry* calculated from different subsets of x-ray structures within different approximations** (c.f., Figure 5). A slightly longer helical coherence length of dodecamers may result from more constraints on their packing in crystals (c.f., Figure S2).